Effect of Coal Filler on the Properties of Soy Protein Plastics

Wang Guang-Heng, Zhou An-ning, Hu Xiao-Bing

Department of Chemistry and Chemical Engineering, Xi'an University of Science and Technology, Xi'an 710054, People's Republic of China

Received 28 August 2005; accepted 10 February 2006
DOI 10.1002/app.24277
Published online in Wiley InterScience (www.interscience.wiley.com).

ABSTRACT: The influence of ultrafine coal filler (UFC) content on tensile properties, water absorption, and biodegradability of soy protein plastics were investigated. The addition of UFC in the soy protein plastics, with different content of glycerol as a plasticizer, was at different ratio varying from 10:0 to 6:4. Blend sheets of the soy protein composites were prepared by the compression molding processing. The results show that, with 23.08 wt % glycerol, the tensile strength and elongation at break for the soy protein sheet with coal filler (range from 5 to 30 parts) can be enhanced as compared with nonfilled soy protein plastics. Water resistance of the soy protein plastics improves with the increase in UFC content. The derivative thermogravimetry (DTG) curves indicate a double-stage degradation process for defatted soy flour (SPF), while three-stage degradation process for soy plastics and the soy protein composites. FT-IR, XPS, and SEM were applied to study the interfacial interaction between coal macromolecules and soy protein molecules in UFC filled soy protein plastics. The results demonstrated that there is strong interfacial interaction in the soy protein plastics caused by the compression molding processing. J Appl Polym Sci 102: 3134–3143, 2006

Key words: biodegradable; blends; fillers; thermogravimetric analysis; plastics

INTRODUCTION

Recently, soy proteins plastics have been considered as petroleum polymer alternatives for their abundant resources, low cost, and super biodegradability. It has been found that the low moisture (<5 wt %) soy protein plastic is tougher than diglycidyl ether of bisphenol-A epoxy resins, and their Young's moduli are higher than that of petrochemical engineering plastics.[1] However, soy protein plastics are brittle and water sensitive. The mechanical properties of soy protein plastics decrease drastically when they contain higher content of water or exposure to moisture.[2] The application of soy protein plastics is limited for this reason. Therefore, chemical and physical modifications, such as aldehyde crosslinking,[3,4] sodium dodecyl sulfate modification,[5,6] blending with other biodegradable polymers,[7–10] and filling with polyphosphate[11,12] and lignin[13,14] fillers, have been used to improve the processability, mechanical properties, and water resistance of soy protein materials. Addition of fillers in soy plastics effectively promotes the strength and water resistance of soy protein plastics.[11,13,14]

Coal is a complex mixture of amorphous organic materials with inorganic material interspersed. The organic geochemistry study show that coal has a macromolecular structure with a molecular phase composed of relatively small molecules associated with the coal matrix. Three-dimensionally crosslinked macromolecular network is supposedly made up of relatively low-weight structure units connected by various types of bonds. The units are made up of cyclic aromatic, hydroaromatic, and heterocyclic carbon structure units connected by covalent bonds (alkyl, etheric, oxygen, and sulfur bridges), noncovalent bonds (Vander Waals forces) and hydrogen bonds. There are various types of active aside groups such as —OH, —COOH, —NH_2 connected on coal molecules.[15] Coals are subject to weathering degradation[16] and biodegradation,[17] especially for low-rank coals,[18] and the degradation products are mainly humic acids.[19,20] These coal-derived humic acids are effective organic matter for soil amelioration.[21–23]

The research and development of coal-filled synthetic polymers can be dated back to 1970s.[24,25] In our laboratory, ultrafine coal powders have been used as functional filler for improving performance of synthetic or natural polymers, especially conductive or degradable composites from coal and polymers.[26,27] In previous work, the effects of soy protein treatment on the biodegradability of coal and oxidized coal were

Correspondence to: A. Zhou (zhouanning2004@yahoo.com.cn).
Contract grant sponsor: Key Project Foundation of Shaanxi Province, China; contract grant number: 2000K-1009.

TABLE I
Properties of UFC

Proximate analysis	
M_{ad}	7.29
A_d	4.27
V_{daf}	36.42
FC_d	60.87
Ultimate analysis	
C_{daf}	81.75
H_{daf}	4.79
O_{daf}	11.95
N_{daf}	1.10
S_{daf}	0.38

studied.[28] The results show that soy protein treatment enhances the biodegradability of coal by increasing humic acids and water-soluble matters in biodegradation products. It reveals the application for biodegradable materials of coal and weathered coal. The objectives of the present study were to study the effects of UFC content on tensile strength, elongation at break, water absorption, thermal degradation, and interfacial interaction of UFC filled soy plastics.

EXPERIMENTAL

Materials

Defatted soy flour (SPF) is a received commercial products provided by Shenghua Vegetable Protein (Henan, China). The contents of protein and moisture in SPF are 51.0% and 4.64%, respectively. Coal is a kind of subbituminous coal (supplied by Shenfu Coal Mine, Shaanxi, China). The coal was pulverized into ultrafine powders in particle size of D_{90} less than 12 μm (UFC). The properties of the coal are given in Table I. The soil sample used to isolate microorganisms was taken from upland field in southern suburb of Xi'an.

The medium used for microorganism isolation contained 0.1 g KH_2PO_4, 0.076 g $K_2HPO_4 \cdot 3H_2O$, 0.04 g $MgSO_4 \cdot 7H_2O$, 1.0 g $(NH_4)_2SO_4$, 0.1 g NaCl, 0.0075 g $CaCl_2$, 1 L distilled water, and 20 g agar agar. Gause medium No. 1 and PDA medium were used to cultivate actinomycete and fungi, respectively. The inorganic salt medium used for the biodegradation test contained, 1.0 g K_2HPO_4, 0.5 g KH_2PO_4, 0.4 g $MgSO_4 \cdot 7H_2O$, 0.0075 g $CaCl_2$, and 1 L distilled water.

Preparation of blend sheets

The blend sheets of SPF and UFC were prepared via compression molding processing using glycerol as plasticizer. Mixtures of SPF and UFC (with UFC of 0, 5, 10, 20, 30, and 40 parts) with different glycerol content (16.67, 23.08, 28.57, and 33.33 wt %) were mechanically mixed at ~4°C. Glycerol was dropped into the mixtures. Subsequently, the mixture was aged at 4°C for 24 h in closed containers previously to the molding processing. The specimens were molded at 140°C and 20 MPa for 5 min and then cooled to ~50°C before removal from the mold to obtain the blend sheets. The composition of the blend sheets is listed in Table II.

Tensile property tests

The tensile properties were examined at room temperature with a KD-50 tensile tester (Shenzhen Kaiqiangli testing instruments, China) according to ASTM D638-91. Test bars (Type 1B) were die-cut from the blend sheets according to standard method ASTM D638-91. The samples were conditioned for 48 h at 23°C and 50% ± 5% relative humidity before testing. The cross-head speed was 50 mm min^{-1}. Tensile strength at maximum load and elongation at break were calculated. The reported results are averages of six samples.

Water absorption measurement

Water absorption was measured by following ASTM standard method, ASTM D570-81. The blend sheets were vacuum-dried at 50°C to constant weight. And then they were cooled in a desiccator, weighed, and submerged in distilled water at 25°C for 2 and 24 h. The extra water on the surface of the sheets after water soaking was removed with a paper towel, and weighed again. Finally, the wet sheets were vacuum-dried at 50°C to constant weight to calculate the water-soluble matter. Water absorption of the blend sheets ($WA_{sheet,}$ %) was calculated according to eq. (1). On the basis of the hypothesis that coal does not absorb water, the water absorption per unit mass of SPF (WA_{sheet}, g H_2O g^{-1} SPF) was calculated according to eq. (2).

$$WA_{sheet} = \frac{W_1 - W_0 + W_S}{W_0} \quad (1)$$

TABLE II
Composition of Soy Protein Sheets

Blend sheets	SPF/UFC/glycerol	Blend sheets	SPF/UFC/glycerol	Blend sheets	SPF/UFC/glycerol	Blend sheets	SPF/UFC/glycerol
SC0–20	100/0/20	SC0–30	100/0/30	SC0–40	100/0/40	SC0–50	100/0/50
SC5–20	95/5/20	SC5–30	95/5/30	SC5–40	95/5/40	SC5–50	95/5/50
SC10–20	90/10/20	SC10–30	90/10/30	SC10–40	90/10/40	SC10–50	90/10/50
SC20–20	80/20/20	SC20–30	80/20/30	SC20–40	80/20/40	SC20–50	80/20/50
SC30–20	70/30/20	SC30–30	70/30/30	SC30–40	70/30/40	SC30–50	70/30/50
SC40–20	60/40/20	SC40–30	60/40/30	SC40–40	60/40/40	SC40–50	60/40/50

$$WA_{SPF} = \frac{W_1 - W_0 + W_S}{W_{SPF}} \quad (2)$$

where W_1 is the weight of the sheet containing water; W_0, the weight of the dry sheet; W_S, the weight of the water-soluble matter; and W_{SPF} is the weight of SPF in the dry sheet. The values presented are averages of three specimens.

Isolation and screening of coculture

A 5-g soil sample was added to a 250 mL Erlenmeyer flask and homogenized with 100 mL distilled water on an oscillator for 15 min. And then 1 mL of appropriate 100-fold dilution of the supernatant was inoculated onto the isolation medium mentioned above and kept at 28°C for 3–5 days. The stock plants of actinomycete and fungi were carefully isolated from the isolation medium and inoculated onto Gause medium No. 1 and PDA medium in 90 mm petri dishes, respectively. The dishes were then kept at 28°C for 7–10 days until the strains covered the whole medium surface.

Aerobic biodegradation test

The actinomycete and fungi were mixed and dispersed in the inorganic salt medium mentioned above at concentration of one plate per 150 mL to prepare coculture medium. 1.000 ± 0.001 g coal sample was then mixed with 150 mL the coculture medium in a 250 mL Erlenmeyer flask, and placed in the incubator in the aerobic biodegradation system[28] (Fig. 1) and kept at 28°C. CO_2-free humidified air passed through each reactor at 20 mL/min. The amount of CO_2 trapped was determined by titration with standardized 0.1*N* HCl.

A total percentage biodegradation for each sample was calculated based on the amount of evolved carbon (mg) divided by the theoretical carbon in each 1-g sample. The theoretical carbon in each sample was determined by the complete combustion of 50-mg sample in a NETZSCH TG 209C thermogravimetric analyzer at 700°C under an atmosphere of oxygen. The exit gas from combustion was passed through a series of CO_2 traps, and the amount of CO_2 liberated was determined by titration. Based on the hypothesis that coal does not generate CO_2 during biodegradation, a total percentage biodegradation of SPF and glycerol for each sample was calculated; in this analysis the theoretical carbon in each sample did not include the carbon from UFC.

Thermogravimetric analysis (TGA)

Specimens were scanned using a NETZSCH TG 209C thermogravimetric analyzer at different heating rates (5, 10, 20°C min^{-1}) with a pure N_2 gas flow of 20 mL min^{-1}. The thermogravimetric data were analyzed suing Kissinger method,[29] and the activation energy (E) was then determined.

Fourier Transform infrared spectroscopy

Fourier Transform infrared spectroscopy (FT-IR) was performed with a Perkin–Elmer Spectrum GX facility with a resolution of 4 cm^{-1}, in the range 4000–400 cm^{-1}.

Scanning electron microscopy

The morphology of the fractured surfaces of tensile specimens of SC0-30 and SC20-30 was observed using a JEOL JSM-6460LV scanning electron microscope (SEM) at an accelerating voltage of 20 kV. The specimens examined were coated with thin layers of gold using an Agar sputter coater to enhance conductivity.

X-ray photoelectron spectroscopy

X-ray photoelectron spectroscopy (XPS) analyses were performed with a Perkin–Elmer PHI 5400 spectrometer using Mg Kα X-ray source (1253.6 eV) operated at 400 W. Samples were dried in a vacuum at 60°C for 24 h before test. Survey scans were collected from 0 to 1000 eV with pass energy of 89.45 eV. A correction for binding energy was made to account for sample charging based on the C1s peak at 285.0 eV. The C1s and N1s peaks were curves resolved using Gaussian line shape.

To study the interfacial interaction between soy protein and coal, a mixture of SPF and UFC (9:1, w/w) was molded into sheet (SPF-UFC) for XPS analysis.

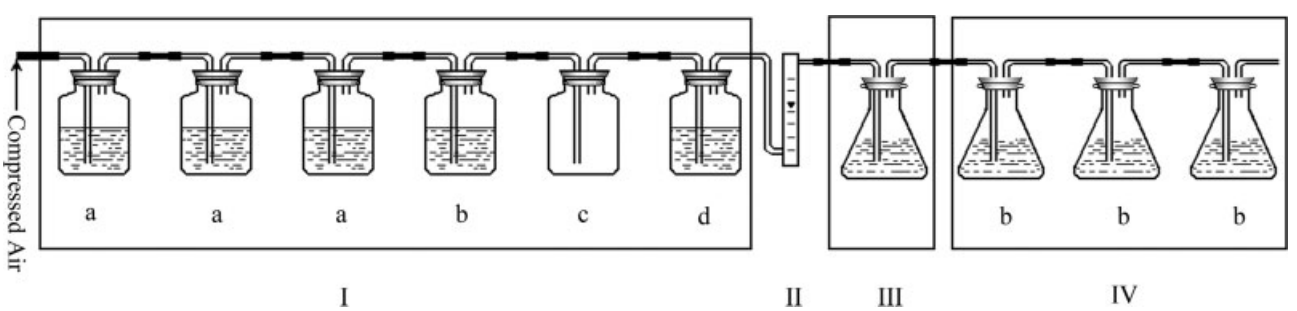

Figure 1 Schematic diagram of aerobic biodegradation system. I, air scrubbing system; II, flow rate control system; III, bioreactor; IV, CO_2 posttraps. a, NaOH; b, $Ba(OH)_2$; c, empty bottle; d H_2O.

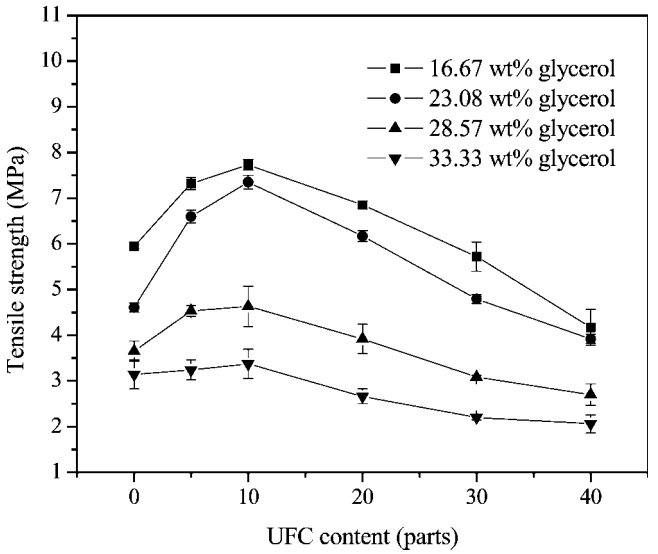

Figure 2 Tensile strength for soy protein sheets.

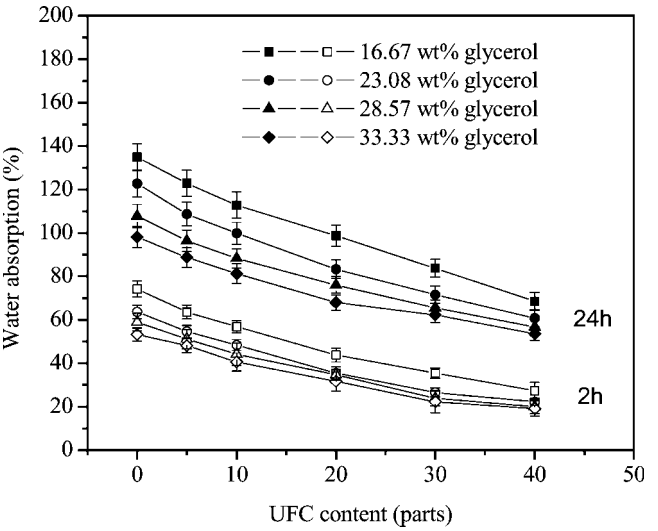

Figure 4 Water absorption of soy protein sheets.

RESULTS AND DISCUSSION

Tensile properties

The effect of UFC content on the tensile properties of the soy protein composites is shown in Figures 2 and 3. The tensile strength (Fig. 2) of the sheets increases with an increase in the UFC content up to 10 parts and then decreases at the same content of glycerol. And the reinforcement effect decreases with the increase of glycerol content. Figure 3 shows the elongation at break of the soy protein sheets. It can be seen that the elongation at break of both unfilled and coal filled sheets sharply decreases with the increase of glycerol. In the glycerol content range from 166.77 to 28.57 wt %, the elongation at break of the sheets with 5 parts coal filler are higher than that of unfilled sheets, and then decreases steadily on further increasing the content of UFC up to 40 parts.

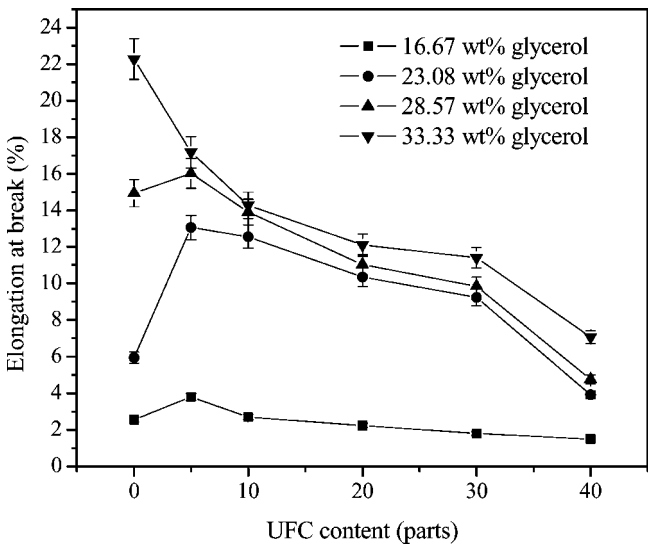

Figure 3 Elongation at break for soy protein sheets.

It has been found that the UFC content ranging from 5 to 30 parts results in the simultaneous enhancement of tensile strength and elongation at break for the blend sheets with 23.08 wt % glycerol. These results indicate that glycerol mainly acts as a plasticizer in the blend sheets.

Water absorption

The water absorption of the blend sheets with different glycerol content decreases with the increase of UFC, as shown in Figure 4. This trend is much clearer in the case of the water absorption per unit mass of SPF (Fig. 5), which was calculated based on the hypothesis that coal does not absorb water. Generally, hydrogen bands can be formed between soy protein molecules and glycerol, then inhibit soy protein absorb water. Thus the water absorption of the sheets decreases with the increase of glycerol. It was supposed from the results that some interactions among hydrophilic groups in coal molecules and soy protein molecules have been occurred during the compression molding processing.

Thermogravimetric analysis

The thermogravimetric/derivative thermogravimetry (TG/DTG) curves for SPF, SC0-30, SC10-30, and SC20-30 are shown in Figure 6. Table III summarizes the thermogravimetric parameters for the degradation of the above samples. For SPF powder, the weight loss up to $\sim 200^{\circ}C$ is related to the loss of adsorbed and bound water. The degradation of SPF undergoes a double-stages process. The first stage began at $\sim 202^{\circ}C$, reached the maximum decomposition rate at $303^{\circ}C$, and ended at ca $350^{\circ}C$ [Fig. 6(a), Table III]. The mass loss in this period is due to the decomposition of soy protein.[30] After the first period decomposition the char is about 46.39% (Table III). The two mass loss peaks observed in DTG

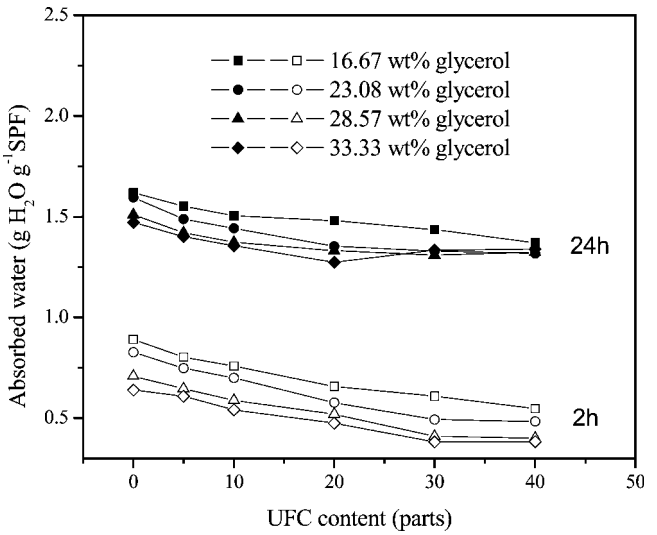

Figure 5 Water uptake of SPF in the soy protein sheets.

curve indicate that there are two main ingredients with different thermal stability in SPF. The second stage (350–850°C) is attributed to the further pyrolysis of the char to release volatiles. For SC0-30, three-states degradation process is observed from the DTG curve [Fig. 6(b)]. The initial degradation temperature for the first stage decreases to 168°C, and a sharp peak at ~195°C is observed in the DTG curve [Fig. 6(b), Table III]. This period is mainly due to the evaporation of glycerol.[31] The mass loss of this period is 35.30%, which is higher than the glycerol content 23.08%. These results indicated that the partial decomposition of protein in SC0-30 sheet has been taken place in this period. Chen and Zhang[31] also found the similar result. The second stage began at ~261°C, arrived the maximum decomposition rate at 303°C, and ended at ~351°C. This stage corresponds to the first degradation stage of SPF. The mass loss is due to the decomposition of protein. After this period the char is about 37.52%, which is slightly higher than the calculated value (Table III). The increased thermal stability of protein is due to the interaction formed between protein molecules and glycerol during compression molding process.[31] While the third stage of the further pyrolysis of the char ended at ~630°C, indicating that the thermal stability of the char is decreased compared to SPF. The reason for this

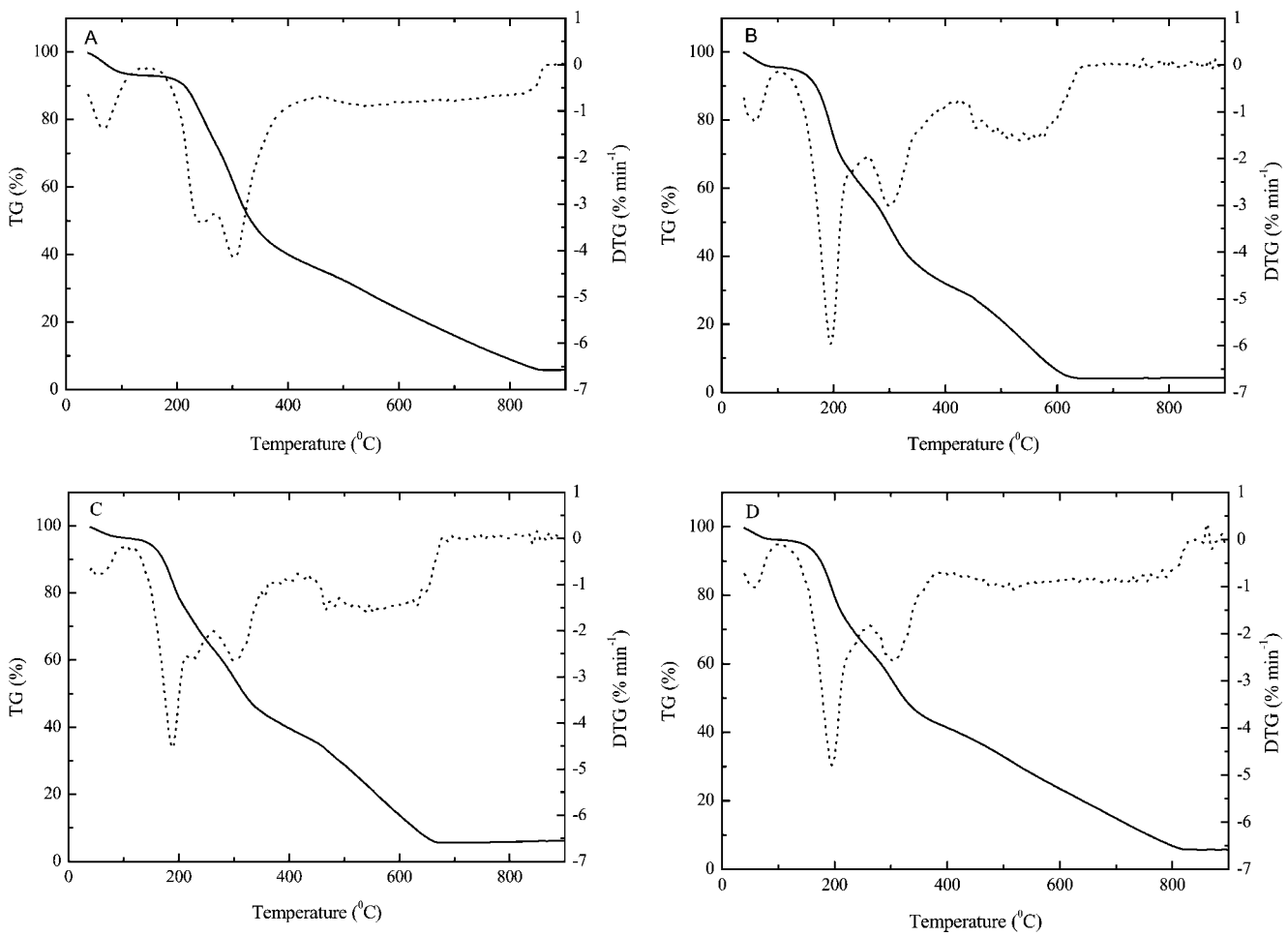

Figure 6 TG (solid line) and DTG (dotted line) curves for (a) SPF powder, (b) SC0-30, (c) SC10-30, and (d) SC20-30 plastics measured at a heating rate of 10°C min^{-1} under nitrogen atmosphere.

TABLE III
Thermogravimetric Parameters for the Decomposition of SPF, and Soy Protein Plastics

Sample	T_i[a] (°C)	T_{max}[b] (°C)	E_1[c] (kJ mol^{-1})	E_2[d] (kJ mol^{-1})	Residue[e] (%)
SPF	202	303	127	172	46.39
SC0	168	195	78	149	37.52
SC10	164	188	92	163	44.61
SC20	169	195	97	169	45.56

[a] Initial temperature of decomposition.
[b] Temperature at maximum degradation rate.
[c] The apparent activation energy for the temperature range of 180–210°C.
[d] The apparent activation energy for the temperature range of 280–310°C.
[e] Values determined at 350°C at a heating rate of 10°C min^{-1}.

decrease is that the continuous network of the protein matrix was disrupted by the small molecule of glycerol,[31] hence further crosslinking reactions of the reactive side groups of amino acids in protein were restricted during pyrolysis.[30] The degradation processes of SC10-30 and SC20-30 are similar to that of SC0-30. The initial degradation temperature and mass loss peaks of the first two degradation stages of SC10-30 and SC20-30 are close to those of SC0-30; but the char residues at 350°C for SC10-30 and SC20-30 are slightly higher than the calculated values (Table III). Furthermore, the final decomposition temperature of the third stages for the further pyrolysis of the char increases with the increase of UFC (Table III) as compared to that of SC0-30, indicating that the thermal stability of the char is increased.

To further investigate the effect of UFC on the degradation behavior of the soy protein composites, the apparent activation energies (E) at degradation temperature range of 180–210°C (E_1) and 280–310°C (E_2) were determined using Kissinger method[29] (Table III). The E values for SC10-30 and SC20-30 are higher than that of SC0-30, and increase as a function of the UFC content. The E_1 and E_2 values shift from 78 and 97 kJ mol^{-1} for SC0-30 sheet to149 and 169 kJ mol^{-1} for SC20-30 sheet, respectively. The results indicate that UFC can restrict the evaporation of glycerol due to adsorption of glycerol on porous coal and enhances the thermal stability of the soy protein composites.

Interfacial interaction

The interfacial interaction between coal and soy protein was investigated by XPS and FT-IR. The FT-IR spectra for UFC, SPF, SC0-30, and SC20-30 are shown in Figure 7. Figure 8 presents the XPS data and deconvolution results for UFC powder [Fig. 8(a) C1s, b N1s], SPF powder [Fig. 8(c) C1s, d N1s], SPF-UFC sheet [Fig. 8(e) C1s, f N1s], and SC20-30 sheet [Fig. 8(g) N1s].

In the FT-IR spectrum for UFC [Fig. 7(a)], the broad absorption band observed in the range of 3680–3300 cm^{-1} is attributed to free and bounded —OH and —NH groups in coal. The adsorption bands between 2970 and 2800 cm^{-1}, and 1780–1700 cm^{-1} are attributed to the aliphatic —CH, —COOH and C=O groups.[32] The C 1s spectrum from a freshly ground surface of UFC is shown in Figure 8(a). The peaks at binding energies of 248.8, 286.1, 287.0, and 288.8 are assigned to **C**—H (or **C**—C), **C**—O, **C**=O (or O—**C**—O) and **C**OOH (or **C**OO$^-$) groups.[33–35] These results indicate that UFC is a kind of low-rank coal. Generally, low-rank coal is easily to be degraded by microorganisms.[18] The results of deconvolution of the N 1s signal for UFC, shown in Figure 8(b), clearly indicate that the greatest amount of nitrogen occurs in UFC as quaternary nitrogen (NH_3^+ or C—**N**H_2^+),[36,37] followed by pyrrolic,[36] and then pyridinic types.[36] The quaternary nitrogen is easier for microorganisms to use as nitrogen resources than pyrrolic and pyridinic species.

The FT-IR spectrum for SPF [Fig. 7(b)] shows absorption bands related to C=O at 1654 cm^{-1} (amide I), N—H at 1542 cm^{-1} (amide II), the C—N and N—H (amide III) at 1242 cm^{-1}.[30] And the broad absorption band observed in the range of 3600–3000 cm^{-1} is also attributed to free and bounded —OH and —NH groups. The **C**—N: N—**C**O ratio is 1.49 in SPF

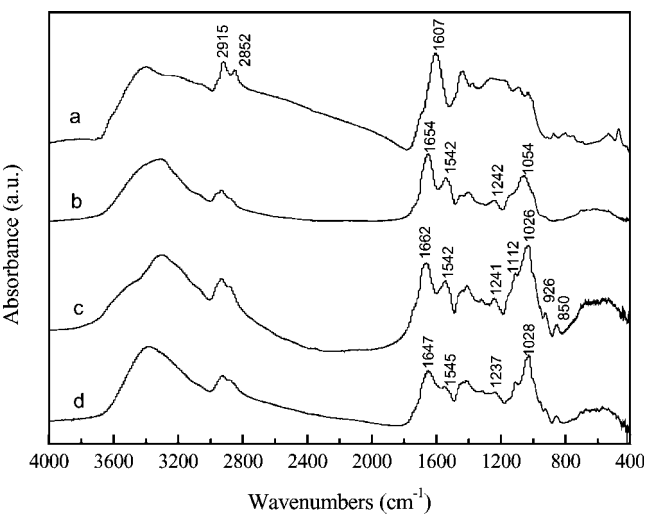

Figure 7 FT-IR spectra for (a) UFC, (b) SPF, (c) SC0-30, and (d) SC20-30.

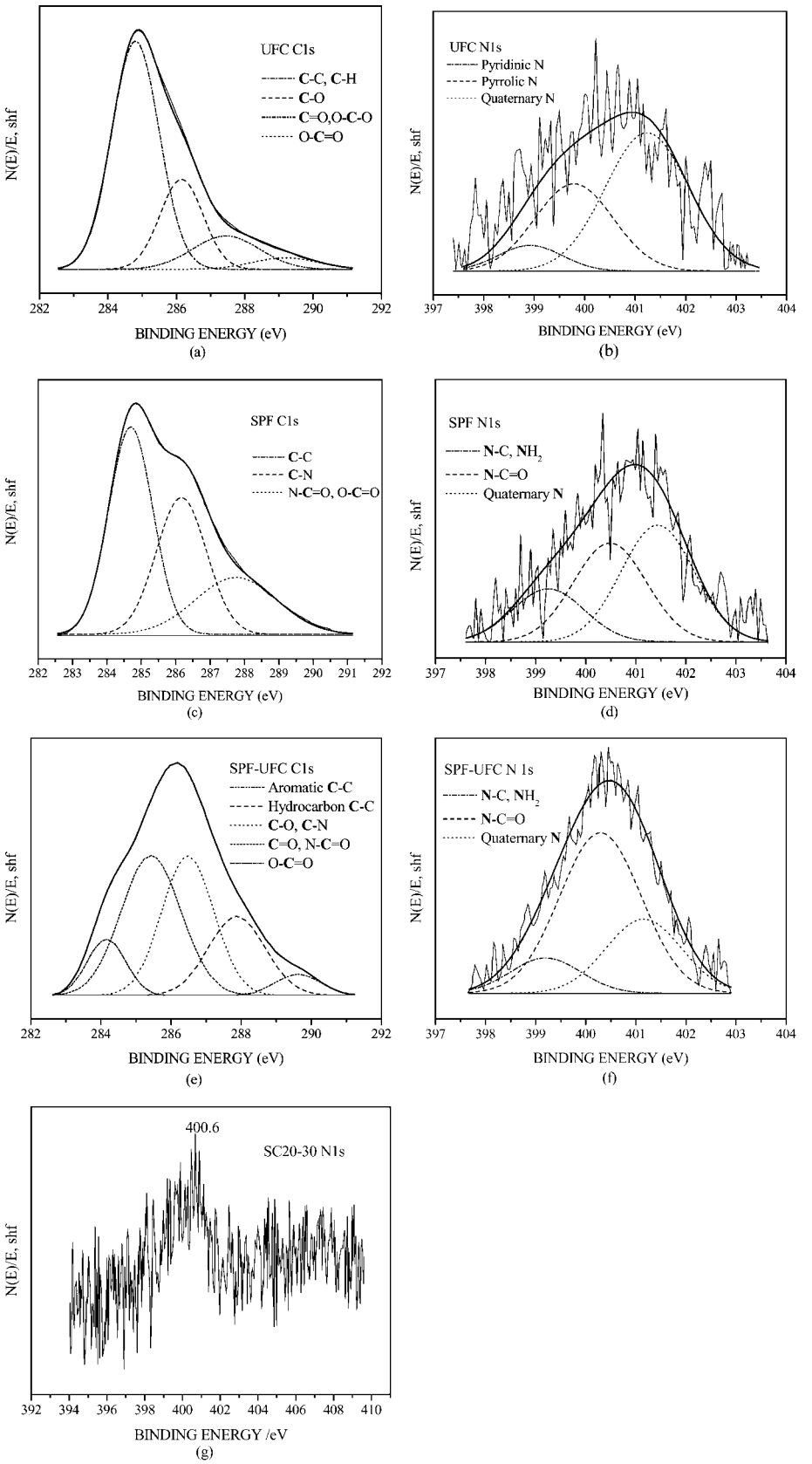

Figure 8 XPS C1s and N1s spectra and curve resolution into different components for UFC, SPF, SPF-UFC, and SC20-30. (a) UFC C1s, (b) UFC N1s, (c) SPF C1s, (d) SPF N1s, (e) SPF-UFC C1s, (f) SPF-UFC N1s, (g) SC20-30 N1s.

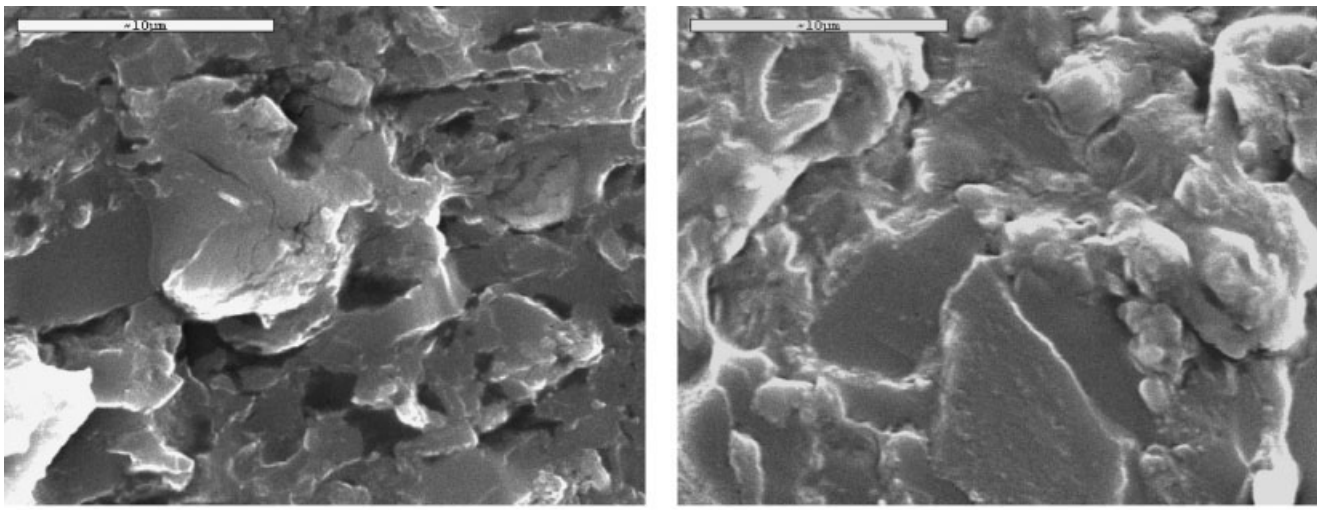

Figure 9 SEM images for the fractured surface of (a) SC0-30 and (b) SC20-30.

[Fig. 8(c)].[38,39] It is relatively higher than the ratio of amide linkage (—**C**—N—**C**O—, 1:1). And the XPS N1s spectrum [Fig. 8(d)] for SPF demonstrate emergence of C—**N** and —**N**H_2 peaks at 399.2 eV.[40] These results suggest the existence of free NH_2 in SPF. In addition, the peak at 401.5 eV is attributed to ionic bonds in soy protein molecules formed between the end groups of —NH_2 and —COOH. During compression molding, the hydrogen bonds and ionic bonds that maintain the spatial structure of protein will be destroyed to some extent, and then parts of the —NH_2 and —COOH groups are librated.

In the case of SC0-30 [Fig. 7(c)], the characteristic absorption peaks for glycerol are clearly observed at 1112, 1026, 925, and 850 cm^{-1}.[41] These indicate that part of glycerol molecules presents in free form.[31] The presence of free glycerol also can be found in SC20-30 sheet [Fig. 7(c)]. These demonstrate that glycerol is mainly act as a plasticizer in soy protein plastics both with and without coal filler.

There are reactive functional groups in coal macromolecule, such as —OH, —COOH, and aliphatic groups, based on the FT-IR and XPS analysis. Therefore, intermolecular interactions (such as hydrogen bonding, dipole–dipole, and charge–charge) are expected to form among the active polar amino side chains of soy protein and coal macromolecules. To study the interfacial interaction between coal and soy protein, the fracture of blend sheet SPF-UFC (SPF:UFC = 9:1 w/w) was analyzed by XPS. The C 1s spectrum of SFU-UFC is shown in Figure 8(e). It demonstrates a hydrocarbon peak at 285.4 eV, an aromatic carbon peak at 284.4 eV[42] and a small portion of COOH (4.13%). In the N 1s spectrum of SPF-UFC [Fig. 8(f)], the nitrogen from UFC is almost negligible, because its content is much lower than that from soy protein. Thus the nitrogen species mainly reveal the presence of nitrogen in SPF after compression molding with UFC. Comparing with the N 1s spectrum of SPF, the percent of free NH_2 in SPF-UFC obviously decreases. Meanwhile, the amide group increases. But the increase of newly formed amide linkages cannot be identified in the XPS N1s signal for the fracture of SC20-30 [Fig. 8(g)]. The spectrum shows a gross peak at 400.6 eV. The change of N species is difficult to identify. The possible reason for this may be the high content of glycerol in the fracture of SC20-30.

In the FT-IR spectrum for SC20-30 [Fig. 7(d)], the intensity of the absorption related to the amide linkages at 1647 cm^{-1} and the —NH groups at 1545 and 1237 cm^{-1} decrease because of the partially breaking of amide linkages and decrease of —NH, respectively, [Fig. 7(d)]. These results demonstrate that some of the

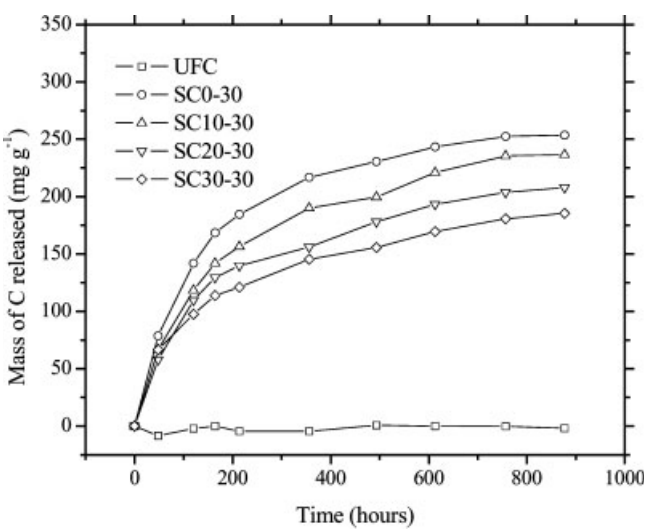

Figure 10 Mass of carbon released by samples exclusively (corrected for presence of coculture).

protein chains are destroyed during compression molding processing. And the —COOH groups in the coal have reacted with the amine groups from the reactive side chains in soy protein to form amide linkages. The new amide linkages, however, are not observed in the FT-IR spectrum of SC20-30 due to the already presence of large number of amide linkages in the backbone of the soy protein. Nevertheless, the shift of the amide I adsorption from 1662 cm^{-1} in SC0-30 to 1647 cm^{-1} in SC20-30 have proved the formation of new amide linkages, because these amide linkages are conjugated with the aromatic rings in coal.

When the content of UFC is relatively low, a core–shell network is formed, in which the UFC ultrafine particles are surrounded by protein chains, resulting in the enhancement of tensile strength and elongation at break. Further increment of coal filler leads to the aggregation of UFC particles, which restricts the formation of the core–shell network mentioned earlier. Hence the tensile properties are decreased. Additionally the linkages of chemical bonding and hydrogen bonding reactions between the hydrophilic groups in protein and coal macromolecules result in the decrease water absorption of the blend sheets.

The SEM images of the fracture surfaces for SC0-30 and SC20-30 sheets are shown in Figure 9. The SC0-30 [Fig. 9(a)] sheet exhibits a relatively smooth fracture. However, the fractured surface of SC20-30 [Fig. 9(b)] is more coarse and ductile. It has been noted that coal particles still are enwrapped in the protein matrix, this is in agreement with the results of interfacial interaction, and indicates there is some miscibility of coal macromolecules and protein macromolecules.

Effect of UFC on biodegradability

To investigate the effect of coal filler on the biodegradability of soy protein plastics, the soy protein plastics with relatively higher tensile properties were used in biodegradation test. UFC powder was used as negative control. SC0-30 (without coal filler) was used as positive control.

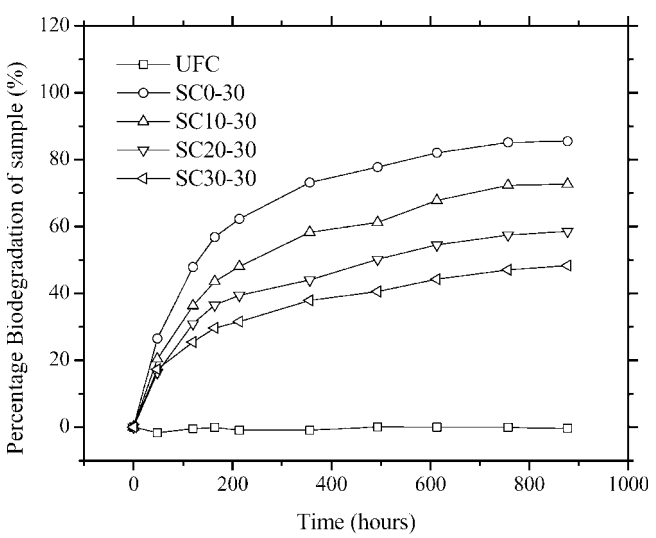

Figure 11 Percent biodegradation of samples by hours.

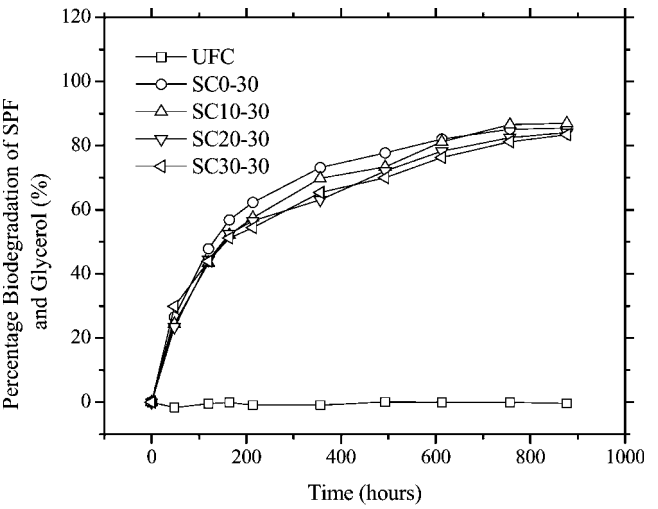

Figure 12 Percent biodegradation of soy protein and glycerol for each sample by hours.

As shown in Figure 10, UFC yields no significant biodegradation during the test. The biodegradation product probably exists in the form of humic acid.[28] Therefore, the total percentage biodegradation of the UFC filled soy protein plastics decreases with the increase of UFC (Fig. 11). More than 85% of SC0-30 is biodegraded after a period of 37 days biodegradation. It is close to the soy protein plastic degraded in soil.[12] Taking into consideration of UFC yielding no significant CO_2, the percentage biodegradation of SPF and glycerol for each sample was calculated (Fig. 12). According to Figure 12, a decreasing percent biodegradation of soy protein and glycerol can be noted for the samples with UFC filler. This may be caused by the inhibition of coal to some microorganisms' metabolism.[28] Nevertheless, all samples show close total percentage biodegradation at the end of biodegradation test. This suggests that, at least, coal had no significantly negative effect on the biodegradation of soy protein and glycerol.

Upon the interfacial interaction analysis, some protein chains are bonded to the surface of coal. The protein can accelerate coal residues converting to humic acids and water-soluble matters hence accelerate the biodegradation of coal.[28]

CONCLUSIONS

Ultrafine coal filler (UFC) reinforced soy protein plastics with higher tensile strength and water resistance were prepared by compression molding processing. The addition of coal in the soy protein plastics can improve the mechanical properties in a large extent. At the same time, enhance the water resistance of the

plastics. The thermal stability also increases with an increase of UFC content, evidencing by the apparent activation energy shifted from 78 and 97 kJ mol^{-1} for SC0-30 sheet to149 and 169 kJ mol^{-1} for SC20-30 sheet at degradation temperature range of 180–210°C and 280–310°C, respectively. The strong interactions between coal and soy protein, such as hydrogen bond and amide linkages, are the main reason for the enhancement of mechanical properties and water resistance of the soy protein plastics. As filler, UFC almost not affects the biodegradability of soy protein plastics. Furthermore, the biodegradability of coal can be enhanced, because some protein chains bond to the surface of coal particle.

References

1. Sue, H. J.; Wang, S.; Jane, J. L. Polymer 1997, 38, 5035.
2. Zhang, J.; Mungara, P.; Jane, J. Polymer 2001, 42, 2569.
3. Swain, S. N.; Rao, K. K.; Nayak, P. L. Polym Int 2005, 54, 739.
4. Rhim, J. W.; Weller, C. L. Food Sci Biotechnol 2000, 9, 228.
5. Rhim, J. W.; Gennadios, A.; Weller, C. L.; Hanna, M. A. Ind Crop Prod 2002, 15, 199.
6. Mo, X.; Sun, X. J Polym Environ 2002, 8, 161.
7. Lu, Y. H.; Weng, L. H.; Zhang, L. Biomacromolecules 2004, 5, 1046.
8. Tang, R.; Du, Y.; Zheng, H.; Fan, L. J Appl Polym Sci 2003, 88, 1095.
9. Lodha, P.; Netravali, A. N. J Mater Sci 2002, 37, 3657.
10. Rhim, J. W.; Gennadios, A.; Weller, C. L.; Cezeirat, C.; Hanna, M. A. Ind Crop Prod 1998, 8, 195.
11. Otaigbe, J. U.; Jane, J. J Environ Polym Degrad 1997, 5, 199.
12. Tkaczyk, A. H.; Otaigbe, J. U.; Ho, G. K. L. J Polym Environ 2001, 9, 19.
13. Huang, J.; Zhang, L.; Chen, F. J Appl Polym Sci 2003, 88, 3284.
14. Huang, J.; Zhang, L.; Chen, F. J Appl Polym Sci 2003, 88, 3291.
15. Marzec, A. Fuel Process Technol 2002, 25, 77.
16. Martínez, M.; Escobar, M. Org Geochem 1995, 23, 253.
17. Fakoussa, R. M.; Hofrichter, M. Appl Microbiol Biotechnol 1999, 52, 25.
18. Machnikowska, H.; Pawelec, K.; Podgórska, A. Fuel Process Technol 2002, 77/78, 17.
19. Kurková, M.; Klika, Z.; Kliková, C. Havel J Chemosphere 2004, 54, 1237.
20. Schmiers, H.; Köpsel, R. Fuel Process Technol 1997, 52, 109.
21. Noble, A. D.; Randall, P. J.; James, T. R. Eur J Soil Sci 1995, 46, 65.
22. Van der Watt, H. V.; Barnard, R. O.; Cronje, I. J.; Dekker, J.; Croft, G. J. B.; Van der Walt, M. M. Nature 1991, 350, 146.
23. Glaser, B.; Lehmann, J.; Zech, W. Biol Fertil Soils 2002, 35, 219.
24. Mueller, W. J. Elastomerics 1978, 110, 17.
25. Gorlov, E. G.; Zummerov, S. R.; Paushkin, Ya. M. Solid Fuel Chem 1977, 11, 1.
26. Xiong, S.; Zhou, A.; Ge, L. J Xiangtan Mining Institute 2001, 16, 30 (in Chinese).
27. Cheng, J.; Zhou, A. N.; Ge, L. M. J China Coal Soc 2003, 28, 188 (in Chinese).
28. Wang, G.; Zhou, A.; Guo, R.; Ge, L. Coal Conversion 2005, 28, 5 (in Chinese).
29. Chan, J. H.; Balke, S. T. Polym Degrad Stab 1997, 57, 135.
30. Schmidt, V.; Giacomelli, C.; Soldi, V. Polym Degrad Stab 2005, 87, 25.
31. Chen, P.; Zhang, L. N. Macromol Biosci 2005, 5, 237.
32. Shu, X.; Wang, Z.; Xu, J. Fuel 2002, 81, 495.
33. Grzybek, T.; Pietrzak, R.; Wachowska, H. Fuel Process Technol 2002, 1, 77.
34. Buckley, A. N.; Lamb, R. N. Int J Coal Geol 1996, 32, 87.
35. Gong, B.; Pigram, P. J.; Lamb, R. N. Fuel 1998, 77, 1081.
36. Kozłlowski, M. Fuel 2004, 83, 259.
37. Raymundo-Piñero, E.; Cazorla-Amorós, D.; Linares-Solano, A.; Find, J.; Wild, U.; Schlögl, R. Carbon 2002, 40, 597.
38. Hitchcock, A. P.; Morin, C.; Heng, Y. M.; Cornelius, R. M.; Brash, J. L. J Biomater Sci Polym Ed 2002, 13, 919.
39. Shibata, Y.; Miyazaki, T. J Dent Res 2002, 81, 841.
40. Weng, L. T.; Poleunis, C.; Bertrand, P.; Carlier, V.; Sclavons, M.; Franquinet, P.; Legras, R. J Adhes Sci Technol 1995, 9, 859.
41. Lodha, P.; Netravali, A. N. Ind Crop Prod 2005, 21, 49.
42. Browne, M. M.; Lubarsky, G. V.; Davidson, M. R.; Bradley, R. H. Surf Sci 2004, 553, 155.